

Microstructure Fiber with Extremely High Nonlinearity for Supercontinuum Generation

Pranjol Sen Gupta*, Mohammad Faisal

Department of Electrical and Electronic Engineering, Bangladesh University of Engineering
and Technology

Dhaka-1205, Bangladesh

*pranjolsengupta93@gmail.com

Abstract— In this paper we present a modified hexagonal microstructure optical fiber (MOF) with circular air holes to achieve high nonlinearity as well as low confinement loss. To explore the chromatic dispersion, nonlinear properties and confinement loss, finite element method (FEM) has been used with an anisotropic, circular perfectly matched boundary layer. Throughout the arrangement of circular shaped holes with various diameters, the hexagonal PCF offers high nonlinearity up to $142 \text{ W}^{-1} \text{ km}^{-1}$ at 1550 nm wavelength and chromatic dispersion of $\sim 0 \pm 0.95 \text{ ps/(nm-km)}$ in the range of 1250 to 1610 nm wavelength. This novel MOF with high nonlinearity and low dispersion is suitable for generating supercontinuum in telecommunication band (around 1300 nm and 1550 nm).

Index Terms— MOF, Nonlinearity, Supercontinuum, Dispersion, Finite Element Method

I. INTRODUCTION

A microstructure optical fiber (MOF) incorporates sub-wavelength air holes along the whole length of the waveguide. These MOFs featuring unprecedented properties [1]-[2] have been the subject of continuous research and development efforts for the past ten years and have fulfilled many of their promises that have further accelerated inventions in many sectors. In contrast with conventional fibers, MOF helps us to engineer various properties like birefringence [3], chromatic dispersion [4]-[5], nonlinearity [6]-[7] etc. MOFs support design parameters such as diameter of the air-hole, ring number, and spacing between air-hole to air-hole (the pitch) which enable us to tune those properties mentioned above. Ultra-short pulses are affected by a multitude of nonlinear effects as well as dispersion of fiber. The nonlinear effects can generate new frequencies in the outside region of input pulse spectrum. With sufficient intensity, a phenomenon like spectral broadening is occurred also known as supercontinuum (SC) generation [8] due to high nonlinearity of fiber. Property of the SC generation is particularly dependent upon the position of input pulse relative to the zero dispersion wavelength. SC generation has received great interest in applications like gas sensing, fluorescence lifetime imaging, frequency metrology and optical communication. Telecommunication window is the most preferable window in optical communication because of the minimal level of transmission loss in the fiber. Maintaining very high nonlinearity with tailoring the chromatic dispersion and restraining the losses to a minimum level are essential for SC generation. Index guiding photonic crystal fiber (PCF) offers unique dispersion and higher nonlinearity [8]-[13] that have been outlined up to date

ranging from PCF with defects in core [8], PCF with a triangular lattice [9], with air holes uniformly optimized [10] and PCF having variation in air-hole diameters in cladding [12]. In [8], proposed hexagonal structure has a much lower nonlinearity of $25 \text{ W}^{-1} \text{ km}^{-1}$ at 1300 nm wavelength and $20 \text{ W}^{-1} \text{ km}^{-1}$ at 1550 nm wavelength whether our proposed structure has nonlinear coefficient of $220 \text{ W}^{-1} \text{ km}^{-1}$ and $142 \text{ W}^{-1} \text{ km}^{-1}$ at respective wavelength. In [9], the proposed structure has dispersion value of 2.0 ps/(nm-km) whereas we have achieved a much lower dispersion $\sim 0.95 \text{ ps/(nm-km)}$ in between 1250 to 1610 nm wavelength. PCFs in [10]-[11] have better dispersion attributes but they incorporate many rings to lessen the confinement losses. For instance, Reeves [11] have shown a dispersion lessened MOF with confinement loss of 0.57 dB/m using eleven rings whereas our proposed structure has a confinement loss of 10^{-8} dB/km using only six rings of air-holes. As a result, the modified hexagonal MOF presented in this paper with low dispersion, very high nonlinearity and extremely low confinement loss will be a proper candidate for SC generation. Furthermore, we use silica as a background material without doping.

II. DESIGN OF MOF AND GEOMETRICAL PARAMETERS

By carefully designing ring number, hole diameter and pitch, dispersion and confinement loss can be significantly altered in MOF. Moreover, existence of holes with various diameter in cladding also help to increase nonlinearity. The cross-sectional view of the hexagonal MOF with details is shown in Fig. 1 with core diameter $2a$ and pitch Λ . In our design, we have used four different sized hole diameters and six rings in the cladding. The diameter of the innermost ring is d_1 , the second ring and third ring have a diameter of d_2 and d_3 respectively and the outermost three rings have a diameter of d_4 . The spacing between adjacent air hole rings and distance between holes on the same ring has been kept fixed in whole analysis. Hence, the diameter of the core is $2\Lambda - d_1$. Use of air-hole of uniform diameters result in ultra-flattened dispersion but it will increase confinement loss. So many rings will be required to lessen the loss to a desired level. However, this will create complexities in fabrication with weak structure. In our case, the hexagonal structure with six air hole rings is adequate for obtaining a low dispersion and low confinement loss as well as higher nonlinearity. As PML is suitable for effective absorption boundary conditions [16], a circular PML has been

incorporated to mask backscattering in the simulation domain. Sellmeier equation [17] has been employed for calculating accurate effective refractive index of fused silica.

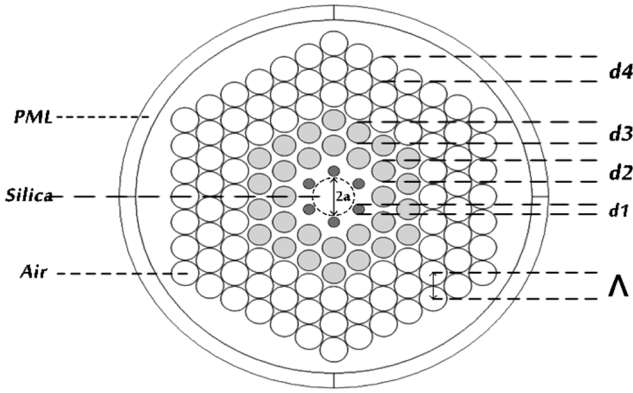


Fig. 1 Geometric Design and parameters of the proposed six ring PCF.

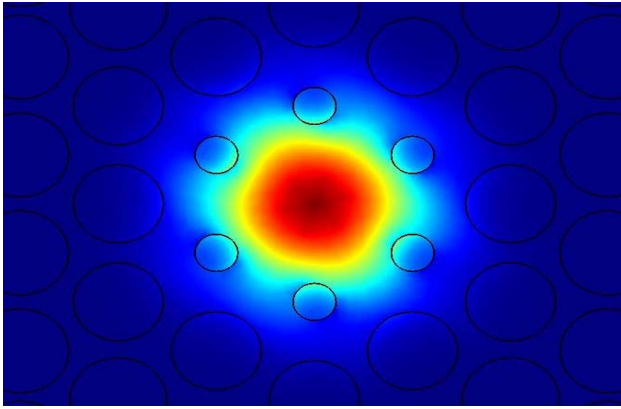


Fig. 2 Power flow distribution inside the proposed MOF at 1.55 μm .

III. NUMERICAL SIMULATION RESULTS AND DISCUSSIONS

We have calculated effective modal index (n_{eff}) and the field distribution of the proposed fiber by using FEM with PML [16]. Power confinement of the proposed structure has been shown in Fig. 2 at 1550 nm wavelength, which clearly reveals the confinement of field in the core. We have used COMSOL multiphysics (v5.0) for numerical simulation. Once n_{eff} is obtained by solving an eigen-value problem with Maxwell's equation by FEM method, the chromatic dispersion parameter (D), effective modal area (A_{eff}), nonlinearity (γ) and confinement loss (L_c) all are calculated by using the following equations [18].

$$D = -\frac{\lambda}{c} \frac{d^2 \text{Re}[n_{\text{eff}}]}{d\lambda^2} \quad (1)$$

$$A_{\text{eff}} = \frac{[\iint |E|^2 dx dy]^2}{\iint |E|^4 dx dy} \quad (2)$$

$$\gamma = \frac{2\pi n_2}{\lambda A_{\text{eff}}} \quad (3)$$

$$L_c = 8.868 \times \text{Im}[k_0 n_{\text{eff}}] \quad (4)$$

Here $\text{Re}[n_{\text{eff}}]$ is the real part of n_{eff} , c is the velocity of light and λ is the wavelength. $\text{Im}[k_0 n_{\text{eff}}]$ is termed as the imaginary part of n_{eff} . Nonlinear refractive index, $n_2 = 2.2 \times 10^{-20} \text{ m}^2/\text{W}$ [19] for silica and E is the electric field inside the fiber derived from Maxwell's equations [18].

In Fig. 3, we have plotted the real part of effective refractive index against wavelength. The real part of refractive index decreases with wavelength. In Fig. 4, we can see the dispersion attributes of the fiber. During whole analysis Λ has been kept at 0.87 μm and the diameter of the innermost ring (d_1) is 0.33 μm and three outermost rings (d_4) is 0.84 μm . The second ring and third ring have a diameter of 0.693 μm and 0.747 μm , respectively. From Fig. 4 it is apparent that at 1300 nm and 1550 nm wavelength there are two zero dispersions and by optimizing the parameters d_1 , d_2 , d_3 , d_4 and Λ , chromatic dispersion in the range of $0 \pm 0.95 \text{ ps}/(\text{nm}\cdot\text{km})$ in between 1250 to 1610 nm wavelength has been achieved.

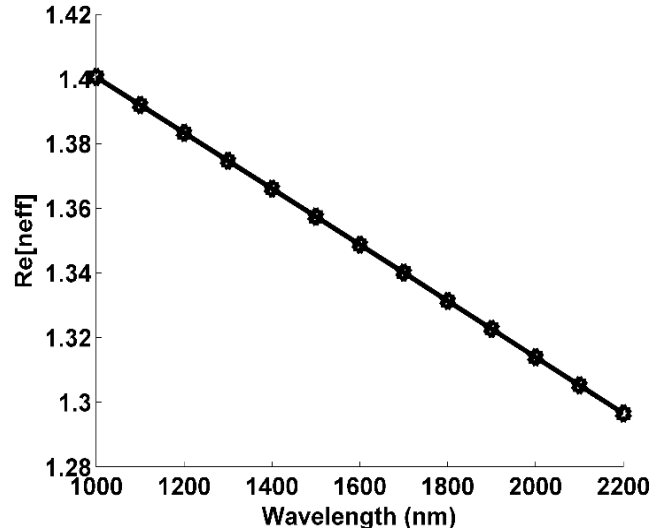


Fig. 3 Real component of effective refractive index.

Next, the design parameters, d_2 and d_3 , have been varied and the effects are shown in Fig. 5 and Fig. 6. First, the diameter of 3rd ring is varied from 0.74 to 0.747 μm while the diameter of 2nd ring is remained unchanged. We can see that the dispersion curve has taken a downward shift. Then in Fig. 6 the diameter of 2nd ring is changed from 0.693 to 0.72 μm and the diameter of 3rd ring is kept at 0.747 μm which results in an upward movement of dispersion curve. It is important to note that other parameters such as pitch and air hole diameter for ring number 1,4,5,6 have been kept fixed. Only the diameters of the 2nd and 3rd ring have been tuned to shape the desired dispersion curve. Though dispersion is lower when diameter of third ring is decreased, consequently, it also reduces the overall wavelength band and shifts zero dispersion wavelength. That's why we have chosen 0.693 μm and 0.747 μm as an optimum diameter for 2nd and 3rd ring, respectively.

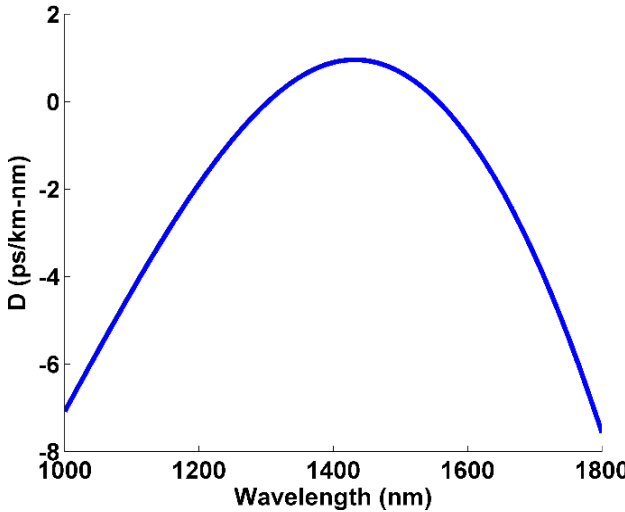


Fig. 4 Dispersion characteristic with optimum value for $\Lambda=0.87 \mu\text{m}$, $d_1=0.33 \mu\text{m}$, $d_2=0.693 \mu\text{m}$, $d_3=0.747 \mu\text{m}$, $d_4=0.84 \mu\text{m}$.

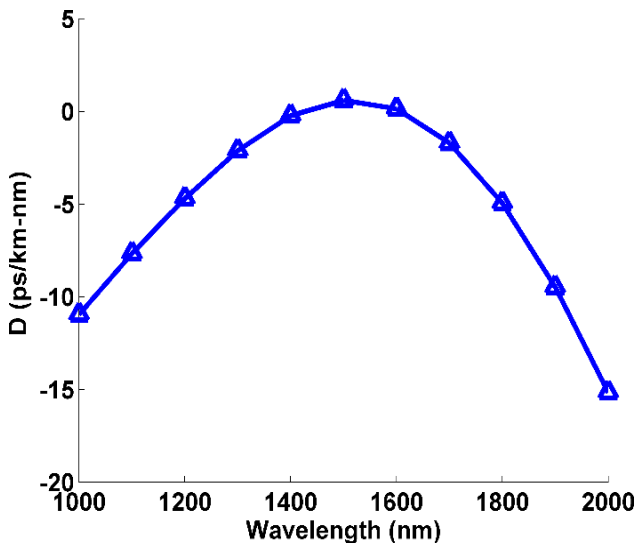


Fig. 5 Dispersion characteristic with optimum value for $\Lambda=0.87 \mu\text{m}$, $d_1=0.33 \mu\text{m}$, $d_2=0.693 \mu\text{m}$, $d_3=0.74 \mu\text{m}$, $d_4=0.84 \mu\text{m}$.

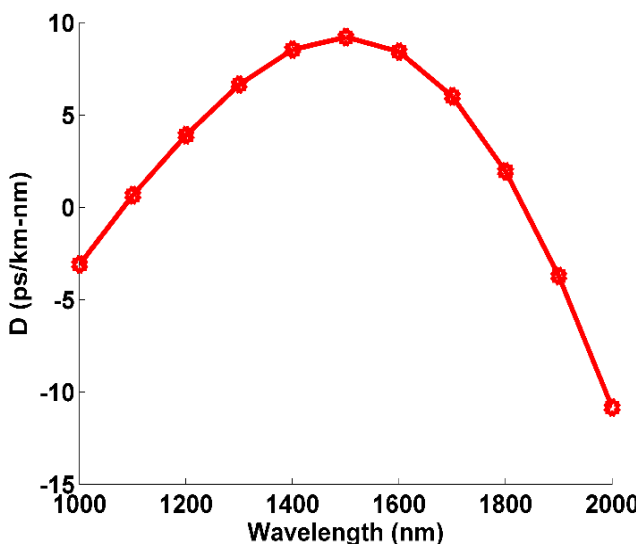


Fig. 6 Dispersion characteristic with optimum value for $\Lambda=0.87 \mu\text{m}$, $d_1=0.33 \mu\text{m}$, $d_2=0.72 \mu\text{m}$, $d_3=0.747 \mu\text{m}$, $d_4=0.84 \mu\text{m}$.

From Eq. (3) it is evident that nonlinearity of a fiber is inversely proportional to effective area of the fiber. Fig. 7 illustrates the variation of effective area with respect to wavelength for different pitch variation. At 1550 nm wave length, effective mode area is $2.85 \mu\text{m}^2$ when pitch is $0.87 \mu\text{m}$. If the pitch is increased to $0.90 \mu\text{m}$, effective area also increases from $2.85 \mu\text{m}^2$ to $3.1 \mu\text{m}^2$ and effective area is $2.37 \mu\text{m}^2$ when pitch is $0.80 \mu\text{m}$, at the same wavelength. In Fig. 8, we have plotted nonlinear co-efficient γ with respect to wavelength for different pitch variation. Because of inverse relation between effective area and nonlinearity, nonlinear coefficient is about $170 \text{ W}^{-1}\text{km}^{-1}$ when pitch is $0.80 \mu\text{m}$ at 1550 nm wavelength. However, with a $0.80 \mu\text{m}$ pitch the overall dispersion is much higher which is not suitable for SC generation. On the other hand, with a pitch of $0.90 \mu\text{m}$ nonlinear coefficient is $132 \text{ W}^{-1}\text{km}^{-1}$ which is lower and not accepted. Finally, the pitch of $0.87 \mu\text{m}$ has been considered as the optimum value that offers nonlinear coefficient of $142 \text{ W}^{-1}\text{km}^{-1}$ at 1550 nm wavelength since here dispersion is zero. We also achieved nonlinearity of $220 \text{ W}^{-1}\text{km}^{-1}$ at 1300 nm wavelength where dispersion is also zero.

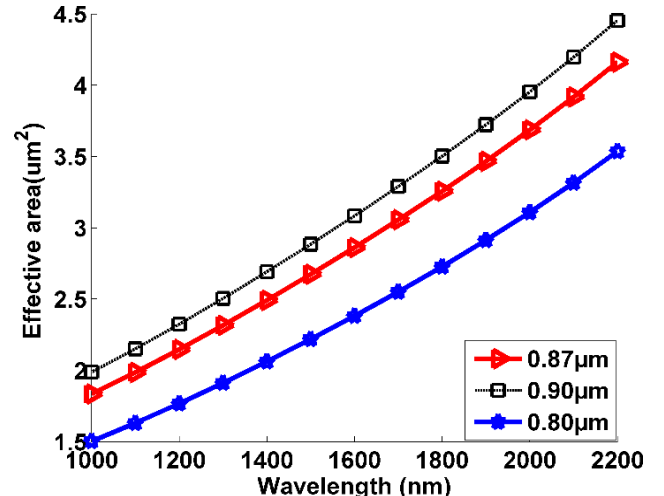


Fig. 7 Effect of pitch variation on effective area with optimum value for $d_1=0.33 \mu\text{m}$, $d_2=0.693 \mu\text{m}$, $d_3=0.747 \mu\text{m}$, $d_4=0.84 \mu\text{m}$.

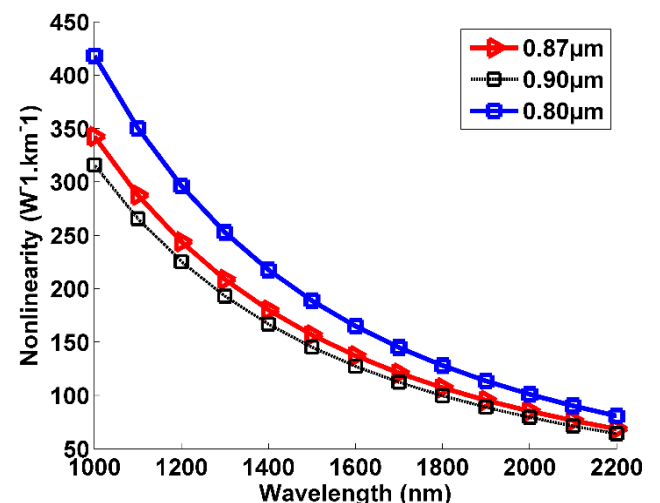


Fig. 8 Effect of pitch variation on nonlinear coefficient with optimum value for $d_1=0.33 \mu\text{m}$, $d_2=0.693 \mu\text{m}$, $d_3=0.747 \mu\text{m}$, $d_4=0.84 \mu\text{m}$.

In Fig. 9, we have shown the effect of ring number on

confinement loss while all the other parameters are kept at their optimum values. With six rings in the cladding, loss in the fiber is nearly 10^{-8} dB/km at 1550 nm operating wavelength, which is extremely low. It is also evident that loss increases as ring number in the cladding is decreased. With six rings, loss is at minimum level and an increase in number of rings do not affect the overall confinement loss significantly. From Fig. 9 it is evident that with seven rings in the cladding confinement loss does not vary much. The diameter of the outer ring has been kept larger in order to avoid leakage loss and poor mode confinement. Only the diameter of first three rings has been altered significantly to get the desired dispersion curve. Now we would like to talk about the possible fabrication of the proposed MOF. Since we are using all circular air holes and hexagonal lattice, we can predict that such simple design could be fabricated using current versatile technology like stack and draw.

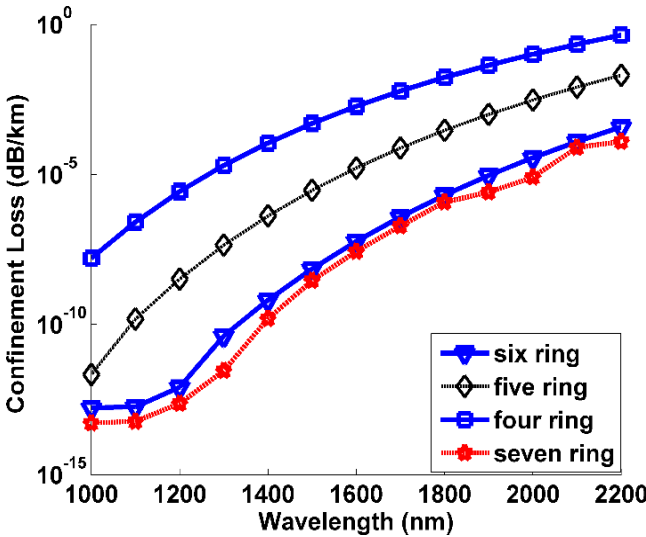


Fig. 9 Effect of ring number on confinement loss with optimum value for $\Delta=0.87 \mu\text{m}$, $d_1=0.33 \mu\text{m}$, $d_2=0.693 \mu\text{m}$, $d_3=0.747 \mu\text{m}$, $d_4=0.84 \mu\text{m}$.

IV. CONCLUSIONS

We have presented a hexagonal MOF with only six rings in cladding and achieved very low dispersion approximately $0\pm0.95 \text{ ps}/(\text{nm}\cdot\text{km})$ in between 1250 and 1610 nm wavelength. We have also achieved two zero dispersion at 1300 and 1550 nm wavelength which is important in the application of supercontinuum generation. We have also shown a lower confinement loss of about 10^{-8} dB/km and very high nonlinearity about $142 \text{ W}^{-1}\text{km}^{-1}$ at 1550 nm wavelength and $220 \text{ W}^{-1}\text{km}^{-1}$ at 1300 nm wavelength. So this proposed design can be a potential candidate for supercontinuum generation.

REFERENCES

- [1] J.K. Ranka, R.S. Windeler, A.J. Stentz, "Optical properties of high delta air-silica microstructure optical fibers," *Opt. Lett.*, vol. 25, no. 1, pp. 796-798, 2000.
- [2] P. St.J. Russell, "Photonic crystal fibers," *Journal of Lightwave Technol.*, vol. 24, no. 12, pp. 4729-4749, 2006.
- [3] J. Ju, W. Jin, and M. S. Demokan, "Properties of a highly birefringent photonic crystal fiber," *IEEE Photon. Technol. Lett.*, vol. 15, no. 10, pp. 1375-1377, Oct. 2003.
- [4] K. Saitoh and M. Koshiba, "Chromatic dispersion control in photonic Crystal fibers: Application to ultra-flattened dispersion," *Opt. Exp.*, vol. 11, no. 8, pp. 843-852, Apr. 2003.
- [5] F. Ge'rome, J. L. Auguste, and J. M. Blondy, "Design of dispersion-Compensating fibers based on a dual-concentric core photonic crystal Fiber," *Opt. Lett.*, vol. 29, no. 23, pp. 2725-2727, Dec. 2004.
- [6] J.C. Knight, T. A. Birk, P. J. St. Russell, and J.P. Sandro, "Properties of photonic crystal fiber and the effective index model," *J. Opt. Soc. Am. A*, vol. 15, no. 3, pp. 748-752, Mar. 1998.
- [7] T. Matsui, J. Zhou, K. Nakajima, and I. Sankawa, "Dispersion-flattened photonic crystal fiber with large effective area and low confinement loss," *J. Lightwave Technol.*, vol. 23, no. 12, pp. 4178-4183, Dec. 2005.
- [8] F. Begum, Y. Namihira, T. Kinjo, S. Kaijage, "Supercontinuum generation in square photonic crystal fiber with nearly zero ultra-flattened chromatic dispersion and fabrication tolerance analysis," *Opt. Comm.*, vol. 284, no. 4, pp. 965-970, 2011.
- [9] A. Ferrando, E. Silvestre, P. Andres, J. Miret, and M. Andres, "Designing the properties of dispersion-flattened photonic crystal fibers," *Opt. Express*, vol. 9, pp. 687-697, 2001.
- [10] A. Ferrando, E. Silvestre, P. Andres, J. J. Miret, and M. Andres, "Nearly zero ultraflattened dispersion in photonic crystal fibers," *Opt. Lett.*, vol. 25, pp. 790-792, 2000.
- [11] W. H. Reeves, J. C. Knight, and P. St. J. Russell, "Demonstration of ultraflattened dispersion in photonic crystal fibers," *Opt. Express*, vol. 10, pp. 609-613, 2002.
- [12] K. Saitoh, M. Koshiba, T. Hasegawa, and E. Sasaoka, "Chromatic dispersion control in photonic crystal fibers: application to ultraflattened dispersion," *Opt. Express*, vol. 11, pp. 843-852, 2003.
- [13] K. Saitoh, N. J. Florous, and M. Koshiba, "Ultraflattened chromatic dispersion controllability using a defected core photonic crystal fiber with low confinement losses," *Opt. Express*, vol. 13, pp. 8365-8371, 2005.
- [14] G. Renversez, B. Kuhlmeier, and R. McPhedran, "Dispersion management with microstructured optical fibers: ultraflattened chromatic dispersion with lowlosses," *Opt. Lett.*, vol. 28, pp. 989-991, 2003.
- [15] H. Ademgil and S. Haxha, "Highly birefringent photonic crystal fiber with ultra low chromatic dispersion and low confinement losses," *J. Lightwave Technol.*, vol. 26, no. 4, pp. 441-448, Feb. 2008.
- [16] S. Guo, F. Wu, S. Albin, H. Tai, R.S. Rogowski, "Loss and dispersion analysis of microstructured fibers by finite difference method," *Optics Express*, vol. 12, pp. 3341-3352, 2004.
- [17] I.H. Malitson, "Interspecimen comparison of the refractive index of fused silica," *J. Opt. Soc. Am.*, vol. 55, no. 10, pp. 1205-1209, 1965.
- [18] K. Kaneshima, Y. Namihira, N. Zou, H. Higa, and Y. Nagata, "A unique approach in ultraflattened dispersion photonic crystal fibers containing elliptical air holes," *Opt. Rev.*, vol. 15, pp. 91-96, 2006.
- [19] K. S. Kim, R.H. Stolen, W. A. Reed, and K. W. Quoi, "Measurement of the nonlinear index of the silica core and dispersion shifted fibers," *Opt. Lett.*, vol. 19, no. 4, pp. 257-259, 1994.